result implies that prestin molecules tend to be accumulated in the plasma membrane.

Besides the ring-like structures, a square-shaped structure with a protrusion at its center, four corners of which are indicated by arrowheads, was rarely observed (M, n=4). The side length of the square, i.e., the length between the adjacent corners indicated by arrowheads (M, Fig. 8b), and the diameter of the protrusion were 7.7 and 6.2 nm, respectively. This type of structure is quite similar to that reported by Mio et al. [12]. According to their report on TEM findings, prestin is a bullet-shaped particle with a small protrusion at its center which extends into the cytoplasm. In the present study, we isolated the inside-out plasma membranes of the prestin-transfected CHO cells and then imaged the cytoplasmic faces of such membranes. On this side, we observed ring-like structures, each with a depression at its center and four surrounding peaks, as shown in Fig. 8. The difference may be due to the difference in observation techniques, the main difference being the force applied to prestin molecules. In the present study, the sample was scanned by the cantilever, the spring constant of which was 0.02 N/m. During the scanning, as the distance between the tip of the cantilever and the sample was controlled so as to reduce the amplitude of the cantilever oscillation by approximately 2–5 nm during scanning, the force applied to the sample could be roughly estimated to be approximately 40–100 pN based on Hooke's law if the load applied to the sample is assumed to be static. In reality, however, since the cantilever was oscillated during scanning, this load was more likely dynamic, suggesting that the force applied to the sample was at least two times larger than such estimation. The application of such force to a protein has been reported to deform its structure [24, 30–32]. On the other hand, TEM does not load such force on the sample. Assuming the flexibility of the cytoplasmic protrusion of prestin, the possibility of deformation of this protrusion into its interior during AFM imaging cannot be ruled out.

In the present study, the topological data were continuously obtained in the transversal direction of the AFM image, i.e., left to right of the image along the x axis shown in Fig. 8a, while those in the transversal direction of the image, i.e., top to bottom of the image along the y axis, were intermittent, implying that the data obtained in the transversal direction were more reliable than those in the longitudinal direction. Therefore, all measured sizes were the transversal sizes of the observed structures. Analysis of sizes of the ring-like structures revealed that the frequency distribution of their diameter showed two main Gaussian distributions, the peaks of which were 9.6±0.1 and 13.0± 0.2 nm (shown by red and blue lines, respectively, in Fig. 8c). The sizes of the first and second peaks were consistent with the previously reported size of prestin [12, 14, 15, 17, 18], as shown in Table 1. If we assume that these two peaks correspond to the compact and extended states of prestin, the diameter change of prestin is approximately 3.4 nm. Based on this, the area change of prestin is calculated to be approximately 60.3 nm^2. In the previous study, the area change of prestin was assumed to be approximately 4 nm^2 [33]. This discrepancy probably relates to the diffusibility of prestin in the plasma membrane. The prestin molecules are considered to be diffusible in the lateral plasma membrane of OHCs [34–39]. In addition, in between the intramembrane molecules, including prestin, there are some spaces [13–18]. In such cases, a large extent of the area change in prestin should be dispersed in the plasma membrane, although to what degree the diffusibility and spaces between the molecules contribute to this dispersion is unknown. In such a scenario, the first peak is probably a smaller state of the ring-like structure and the second peak reflects its larger state, suggesting the existence of a compact as well as extended state of prestin.

As shown in Fig. 8c, the second peak showing the extended state of prestin is broader than the first peak showing its compact state. This result implies that the conformational change of prestin is not just a simple expansion change in sphere shape; rather, it is a directional change in the plane of the plasma membrane, e.g., from the compact sphere shape to the extended oval shape.

In the present study, prestin was observed to be a ring-like structure with a valley at its center surrounded by four

Table 1 Size of prestin

Sample	Method	Size (nm)	Reference
Freeze-fracture replica of the p-fracture face of the guinea pig OHC plasma membrane	SEM	10	Forge [14]
Freeze-fracture replica of the p-fracture face of the guinea pig OHC plasma membrane	SEM	11–15 (up to 20)	Kalinec et al. [15]
Cytoplasmic face of the guinea pig OHC plasma membrane	AFM	11–25	Grimellec et al. [17]
Cytoplasmic face of the gerbil prestin-transfected CHO cell plasma membrane	AFM	8–12	Murakoshi et al. [18]
Purified prestin obtained from rat prestin-transfected Sf9 cell membrane fraction	TEM	7.7–9.6	Mio et al. [12]
Cytoplasmic face of the gerbil prestin-transfected CHO cell plasma membrane	Immune AFM	9.6/13.0	This study

SEM scanning electron microscopy

peaks, suggesting a tetrameric structure of prestin. Analysis of the size of this structure demonstrated two peak distributions, implying the existence of the compact- and extended-state prestin. Utilizing the antibodies which label the C-terminal of prestin instead of those of prestin N-terminal used in this study would lead the important data on the oligomeric structure of prestin since the epitope of the C-terminal of prestin is probably exposed compared with that of the N-terminal [10] so that more precise information could be obtained from the immune AFM images. In addition, imaging with less force applied to the sample using a softer cantilever, appropriate chemical fixation of prestin molecules, and/or imaging the purified prestin molecules may contribute to further analysis of the detailed structure of prestin. Subjecting the isolated plasma membrane to a change in electric potential using a patch electrode or changing the composition of the buffer, e.g., increasing the concentration of Cl^- ions, could possibly yield further information about the mechanisms of the conformational change in prestin.

Conclusions

Prestin molecules expressed in the plasma membranes of prestin-transfected CHO cells were labeled with Qdots about 8 nm in height, which were clearly imaged by AFM. Ring-like structures, each with four peaks and one valley at its center, were observed in the vicinity of the Qdots, suggesting that these structures are prestin.

Acknowledgements This work was supported by Grant-in-Aid for Scientific Research on Priority Areas 15086202 from the Ministry of Education, Cultures, Sports, Science and Technology of Japan, Grant-in-Aid for Scientific Research (B) 18390455 from the Japan Society for the Promotion of Science, a Health and Labour Science Research Grant from the Ministry of Health, Labour and Welfare of Japan, Grant-in-Aid for Exploratory Research 18659495 from the Ministry of Education, Culture, Sports, Science and Technology of Japan, a grant from the Human Frontier Science Program, a grant from the Iketani Science and Technology Foundation and a grant from the Daiwa Securities Health Foundation to H.W., Grant-in-aid for JSPS Fellows 19002194 from the Japan Society for the Promotion of Science and Special Research Grants 11170012 and 11180001 from the Tohoku University 21st Century COE Program of the "Future Medical Engineering Based on Bio-nanotechnology" to M.M.

References

1. Brownell WE, Bader CR, Bertrand D, de Ribaupierre Y (1985) Evoked mechanical responses of isolated cochlear outer hair cells. Science 227:194–196
2. Kachar B, Brownell WE, Altschuler R, Fex J (1986) Electrokinetic shape changes of cochlear outer hair cells. Nature 322: 365–368
3. Ashmore JF (1987) A fast motile response in guinea-pig outer hair cells: the cellular basis of the cochlear amplifier. J Physiol 388:323–347
4. Santos-Sacchi J, Dilger JP (1988) Whole cell currents and mechanical responses of isolated outer hair cells. Hear Res 35:143–150
5. Dallos P, Fakler B (2002) Prestin, a new type of motor protein. Nat Rev Mol Cell Biol 3:104–111
6. Dallos P, Evans BN, Hallworth R (1991) Nature of the motor element in electrokinetic shape changes of cochlear outer hair cells. Nature 350:155–157
7. Zheng J, Shen W, He DZ, Long KB, Madison LD, Dallos P (2000) Prestin is the motor protein of cochlear outer hair cells. Nature 405:149–155
8. Zheng J, Long KB, Shen W, Madison LD, Dallos P (2001) Prestin topology: localization of protein epitopes in relation to the plasma membrane. NeuroReport 12:1929–1935
9. Deák L, Zheng J, Orem A, Du GG, Aguinaga S, Matsuda K, Dallos P (2005) Effects of cyclic nucleotides on the function of prestin. J Physiol 563:483–496
10. Navaratnam D, Bai JP, Samaranayake H, Santos-Sacchi J (2005) N-terminal-mediated homomultimerization of prestin, the outer hair cell motor protein. Biophys J 89:3345–3352
11. Zheng J, Du GG, Anderson CT, Keller JP, Orem A, Dallos P, Cheatham M (2006) Analysis of the oligomeric structure of the motor protein prestin. J Biol Chem 281:19916–19924
12. Mio K, Kubo Y, Ogura T, Yamamoto T, Arisaka F, Sato C (2008) The Motor Protein Prestin Is a Bullet-shaped Molecule with Inner Cavities. J Biol Chem 283:1137–1145
13. Arima T, Kuraoka A, Toriya R, Shibata Y, Uemura T (1991) Quick-freeze, deep-etch visualization of the 'cytoskeletal spring' of cochlear outer hair cells. Cell Tissue Res 263:91–97
14. Forge A (1991) Structural features of the lateral walls in mammalian cochlear outer hair cells. Cell Tissue Res 265:473–483
15. Kalinec F, Holley MC, Iwasa KH, Lim DJ, Kachar B (1992) A membrane-based force generation mechanism in auditory sensory cells. Proc Natl Acad Sci U S A 89:8671–8675
16. Souter M, Nevill G, Forge A (1995) Postnatal development of membrane specialisations of gerbil outer hair cells. Hear Res 91:43–62
17. Le Grimellec C, Giocondi MC, Lenoir M, Vater M, Sposito G, Pujol R (2002) High-resolution three-dimensional imaging of the lateral plasma membrane of cochlear outer hair cells by atomic force microscopy. J Comp Neurol 451:62–69
18. Murakoshi M, Gomi T, Iida K, Kumano S, Tsumoto K, Kumagai I, Ikeda K, Kobayashi T, Wada H (2006) Imaging by atomic force microscopy of the plasma membrane of prestin-transfected Chinese hamster ovary cells. J Assoc Res Otolaryngol 7:267–278
19. Iida K, Konno K, Oshima T, Tsumoto K, Ikeda K, Kumagai I, Kobayashi T, Wada H (2003) Stable expression of the motor protein prestin in Chinese hamster ovary cells. JSME Int J 46C:1266–1274
20. Iida K, Tsumoto K, Ikeda K, Kumagai I, Kobayashi T, Wada H (2005) Construction of an expression system for the motor protein prestin in Chinese hamster ovary cells. Hear Res 205:262–270
21. Murakoshi M, Wada H (2008) Atomic force microscopy in studies of the cochlea. In: Walker J (ed) Molecular protocols in auditory research. Humana Press, Totowa, NJ
22. Ziegler U, Vinckier A, Kernen P, Zeisel D, Biber J, Semenza G, Murer H, Groscurth P (1998) Preparation of basal cell membranes for scanning probe microscopy. FEBS Lett 436:179–184
23. Hartmann WK, Saptharishi N, Yang XY, Mitra G, Soman G (2004) Characterization and analysis of thermal denaturation of antibodies by size exclusion high-performance liquid chromatography with quadruple detection. Anal Biochem 325:227–239

24. Hertadi R, Gruswitz F, Silver L, Koide A, Koide S, Arakawa H, Ikai A (2003) Unfolding mechanics of multiple OspA substructures investigated with single molecule force spectroscopy. J Mol Biol 333:993–1002
25. Lärmer J, Schneider SW, Danker T, Schwab A, Oberleithner H (1997) Imaging excised apical plasma membrane patches of MDCK cells in physiological conditions with atomic force microscopy. Pflugers Arch 434:254–260
26. Iida K, Nagaoka T, Tsumoto K, Ikeda K, Kumagai I, Kobayashi T, Wada H (2004) Relationship between fluorescence intensity of GFP and the expression level of prestin in a prestin-expressing Chinese hamster ovary cell line. JSME Int J 47C: 970–976
27. Mitra K, Ubarretxena-Belandia I, Taguchi T, Warren G, Engelman DM (2004) Modulation of the bilayer thickness of exocytic pathway membranes by membrane proteins rather than cholesterol. Proc Natl Acad Sci U S A 101:4083–4088
28. Michalet X, Pinaud FF, Bentolila LA, Tsay JM, Doose S, Li JJ, Sundaresan G, Wu AM, Gambhir SS, Weiss S (2005) Quantum dots for live cells, in vivo imaging, and diagnostics. Science 307:538–544
29. Dong R, Yu LE (2003) Investigation of surface changes of nanoparticles using TM-AFM phase imaging. Environ Sci Technol 37:2813–2819
30. Janovjak H, Kedrov A, Cisneros DA, Sapra KT, Struckmeier J, Muller DJ (2006) Imaging and detecting molecular interactions of single transmembrane proteins. Neurobiol Aging 27:546–561
31. Dietz H, Bertz M, Schlierf M, Berkemeier F, Bornschlogl T, Junker JP, Rief M (2006) Cysteine engineering of polyproteins for single-molecule force spectroscopy. Nat Protoc 1:80–84
32. Cao Y, Li H (2008) How do chemical denaturants affect the mechanical folding and unfolding of proteins? J Mol Biol 375:316–324
33. Dong XX, Iwasa KH (2004) Tension sensitivity of prestin: comparison with the membrane motor in outer hair cells. Biophys J 86:1201–1208
34. Santos-Sacchi J (2002) Functional motor microdomains of the outer hair cell lateral membrane. Pflugers Arch 445:331–336
35. Zhang M, Kalinec F (2002) Structural microdomains in the lateral plasma membrane of cochlear outer hair cells. J Assoc Res Otolaryngol 3:289–301
36. Santos-Sacchi J, Zhao HB (2003) Excitation of fluorescent dyes inactivates the outer hair cell integral membrane motor protein prestin and betrays its lateral mobility. Pflugers Arch 446:617–622
37. de Monvel JB, Brownell WE, Ulfendahl M (2006) Lateral diffusion anisotropy and membrane lipid/skeleton interaction in outer hair cells. Biophys J 91:364–381
38. Organ LE, Raphael RM (2007) Application of fluorescence recovery after photobleaching to study prestin lateral mobility in the human embryonic kidney cell. J Biomed Opt 12:021003
39. Sturm AK, Rajagopalan L, Yoo D, Brownell WE, Pereira FA (2007) Functional expression and microdomain localization of prestin in cultured cells. Otolaryngol Head Neck Surg 136: 434–439

Biochemical and Biophysical Research Communications 389 (2009) 569–574

Contents lists available at ScienceDirect

Biochemical and Biophysical Research Communications

journal homepage: www.elsevier.com/locate/ybbrc

Mutation-induced reinforcement of prestin-expressing cells

Shun Kumano [a], Xiaodong Tan [b], David Z.Z. He [b], Koji Iida [a], Michio Murakoshi [a], Hiroshi Wada [a,*]

[a] Department of Bioengineering and Robotics, Tohoku University, Sendai, Japan
[b] Department of Biomedical Sciences, Creighton University, Omaha, NE, USA

ARTICLE INFO

Article history:
Received 30 August 2009
Available online 6 September 2009

Keywords:
Inner ear
Outer hair cell
Prestin
Electrophysiological property
Somatic motility
Point mutation

ABSTRACT

The motor protein prestin in cochlear outer hair cells is a member of the solute carrier 26 family, but among the proteins of that family, only prestin can confer the cells with nonlinear capacitance (NLC) and motility. In the present study, to clarify contributions of unique amino acids of prestin, namely, Met-122, Met-225 and Thr-428, to the characteristics of prestin, mutations were introduced into those amino acids. As a result, NLC remained unchanged by both replacement of Met-122 by isoleucine and that of Thr-428 by leucine, suggesting that those amino acids were not important for the generation of NLC. Surprisingly, the replacement of Met-225 by glutamine statistically increased NLC as well as the motility of prestin-expressing cells without an increase in the amount of prestin expression in the plasma membrane. This indicates that Met-225 in prestin somehow adjusts NLC and the motility of prestin-expressing cells.

Introduction

Prestin is the motor protein expressed in the plasma membrane of outer hair cells (OHCs) [1]. A voltage-dependent conformational change of prestin in the plasma membrane is believed to induce OHC electromotility, which is known to be a key element of cochlear amplification [2]. OHCs as well as culture cells engineered to express prestin show electromotility [3], supporting the idea that prestin is the origin of such motility. Although prestin is regarded as one of 11 members of the solute carrier 26 (SLC26) family [4], prestin is the only member of that family which can confer the cells with motility. Nonlinear capacitance (NLC) observed in prestin-expressing cells, which is highly associated with their motility, is often measured for the analysis of prestin activity [5]. To date, several studies on prestin have been performed for its characterization. Mutational studies on prestin have indicated the importance of its N-terminal and C-terminal cytoplasmic domain, identified its glycosylation sites and phosphorylation sites, etc. [6–11], and electron microscopy and atomic force microscopy have revealed the shape of prestin [12,13]. Despite such studies, how prestin confers the cells with motility and NLC has remained unknown.

As conferring cells with motility and NLC is the specific function of prestin in the SLC26 family, unique amino acids in prestin are considered to realize such function. In the present study, to clarify the contributions of such unique amino acids to the characteristics of prestin, point mutations were introduced into those amino acids which were selected by the comparison of the amino acid sequences among the SLC26 proteins. The characteristics of the prestin mutants were then compared with those of wild-type prestin (WT).

Materials and methods

Multiple alignment of the amino acid sequence of the SLC26 family proteins. To select amino acids which are unique in prestin among the SLC26 family, multiple alignment using genes of 11 members of that family was performed by use of the ClustalX Multiple Sequence Alignment Program [14]. In the result of the alignment, the transmembrane domains of prestin in its predicted membrane topology [11] were focused on, as N- and C-terminal cytoplasmic domains have already been well investigated [6–8]. In those domains, the amino acids of prestin were compared with those at corresponding positions of the other SLC26 proteins. By such comparison, we attempted to identify the positions of amino acids where the majority of the SLC26 proteins have the same amino acids but prestin has different amino acids. Such amino acids in prestin were considered to be unique.

Abbreviations: NLC, nonlinear capacitance; OHCs, outer hair cells; SLC26, solute carrier 26; WT, wild-type prestin; FBS, fetal bovine serum; WGA, wheat germ agglutinin; DBcGMP, N^2,2′-*O*-dibutyrylguansine 3′,5′-cyclic monophosphate sodium salt hydrate.

* Corresponding author. Address: Department of Bioengineering and Robotics, Tohoku University, 6-6-01 Aoba-yama, Sendai 980-8579, Japan. Fax: +81 22 795 6939.

E-mail addresses: kumano@wadalab.mech.tohoku.ac.jp (S. Kumano), xiaodong Tan@creighton.edu (X. Tan), davidhe@creighton.edu (D.Z.Z. He), iida@wadalab.mech.tohoku.ac.jp (K. Iida), michio@wadalab.mech.tohoku.ac.jp (M. Murakoshi), wada@cc.mech.tohoku.ac.jp (H. Wada).

0006-291X/$ - see front matter © 2009 Elsevier Inc. All rights reserved.
doi:10.1016/j.bbrc.2009.09.016

Construction of prestin mutant genes. Three genes of prestin mutants, namely, genes of M122I, M225Q and T428L, were constructed by overlap PCR. Constructed prestin mutant genes were ligated into mammalian expression vector pIRES-hrGFP-1a (Stratagene, La Jolla, CA). In addition, to detect prestin by antibodies in immunofluorescence staining and Western blotting, genes expressing the prestin mutants, the C-terminus of which was fused to FLAG-tag, were generated. Such genes were also ligated into the expression vector. The sequences of the constructed genes were confirmed by an automated DNA sequencer (Applied Biosystems, Foster City, CA).

Cell culture and transfection. HEK293 cells were cultured in RPMI-1640 medium (Sigma–Aldrich, St. Louis, MO) supplemented with culture medium consisting of 10% fetal bovine serum (FBS), 100 U/ml penicillin and 100 μg/ml streptomycin at 37 °C with 5% CO_2. One hour before transfection, the culture medium was changed to RPMI-1640 medium supplemented only with 10% FBS. The expression vectors were transfected into HEK293 cells using Fugene HD Transfection Reagent (Roche, Indianapolis, IN) according to the manufacturer's instructions.

Measurement of nonlinear capacitance. NLC in prestin-transfected HEK293 cells, which is commonly used for the evaluation of the function of prestin, was measured by the whole-cell patch-clamp method 36–48 h after transfection, as described previously [15]. The membrane capacitance recorded from the transfected cells was fitted with the first derivative of the Boltzmann function [5],

$$C_m(V) = C_{lin} + \frac{Q_{max}}{\alpha e^{\frac{V-V_{1/2}}{\alpha}}\left(1+e^{\frac{V-V_{1/2}}{\alpha}}\right)^2}, \quad (1)$$

where C_{lin} is the linear capacitance, which is proportional to the membrane area of the cells, Q_{max} is the maximum charge transfer, V is the membrane potential and $V_{1/2}$ is the voltage at half-maximal charge transfer. In Eq. (1), α is the slope factor of the voltage-dependent charge transfer and is given by

$$\alpha = kT/ze, \quad (2)$$

where k is Boltzmann constant, T is absolute temperature, z is valence and e is electron charge. When the NLC curves of the prestin mutants were compared with that of WT, the normalized NLC $C_{nonlin/lin}$ was defined as

$$C_{nonlin/lin}(V) = \frac{C_{nonlin}}{C_{lin}} = \frac{(C_m(V) - C_{lin})}{C_{lin}}, \quad (3)$$

where C_{nonlin} is the nonlinear component of the measured membrane capacitance. In addition, $C_{nonlin/lin}(V)$ was divided by the maximum $C_{nonlin/lin}(V)$ of WT and termed relative $C_{nonlin/lin}(V)$. To evaluate the maximum charge transfer of prestin in the unit plasma membrane, Q_{max}, which is the maximum charge transfer of prestin in whole plasma membrane, was normalized by C_{lin} and designated as charge density.

Motility measurement. Electromotility of the prestin mutant-expressing cells was compared with that of WT-expressing cells using a microchamber configuration 36–48 h after transfection. The motility measurement in such configuration was performed as described previously [16]. In the present study, the electrical stimulus was a 100-Hz sinusoidal voltage burst of 100 ms duration. Voltage commands of ±400 mV were used. Since approximately 50% of the cells were inserted into the microchamber, the resultant voltage drops on the extruded segment were estimated to be 50% of the voltage applied, or ±200 mV [17].

Western blotting. The amount of WT and that of its mutant in transfected cells were evaluated by Western blotting. Forty-eight hours after transfection, 5×10^4 cells were dissolved in SDS sample buffer and used for SDS–PAGE and Western blotting. A prestin band was detected by anti-FLAG mouse monoclonal antibody (Sigma–Aldrich) and HRP-conjugated anti-mouse IgG antibody (Cell Signaling Technology, Beverly, MA). In addition, a β-actin band was detected by anti-β-actin antibody (Sigma–Aldrich) and HRP-conjugated anti-mouse IgG antibody. Those bands were visualized by enhanced chemiluminescence using an ECL Western blotting detection kit (GE Healthcare Bio-Science AB). Western blotting images were obtained with a luminescent image analyzer (Chem-iDoc XRS, Bio-Rad Laboratories, Hercules, CA) and the band intensity was then analyzed. To eliminate the effects of the difference in the concentration of proteins between samples on the comparison of the band intensity, the intensity of the bands in WT and M225Q was normalized by that of β-actin, which is generally used as a control protein. Afterwards, relative intensity was obtained by dividing the normalized intensity of the WT band and that of the M225Q band by the average of the normalized intensity of the WT band.

Immunofluorescence experiment. The localization of WT and that of its mutant in transfected cells were investigated by immunofluorescence staining 48 h after transfection. Plasma membranes of the cells were stained with wheat germ agglutinin (WGA)-Alexa Fluor 633 conjugate (Invitorogene), which has been used for a plasma membrane marker as well as a Golgi body marker. After fixation of the cells with 4% paraformaldehyde and blocking by a buffer consisting of 50% Block Ace (Dainippon Pharmaceutical, Osaka, Japan) and 50% fetal bovine serum, prestin was stained by anti-FLAG antibody (Sigma–Aldrich) in PBS with 0.1% saponin solution and TRITC-conjugated anti-mouse IgG antibody (Sigma–Aldrich) in PBS with 0.1% saponin solution. The stained cells were

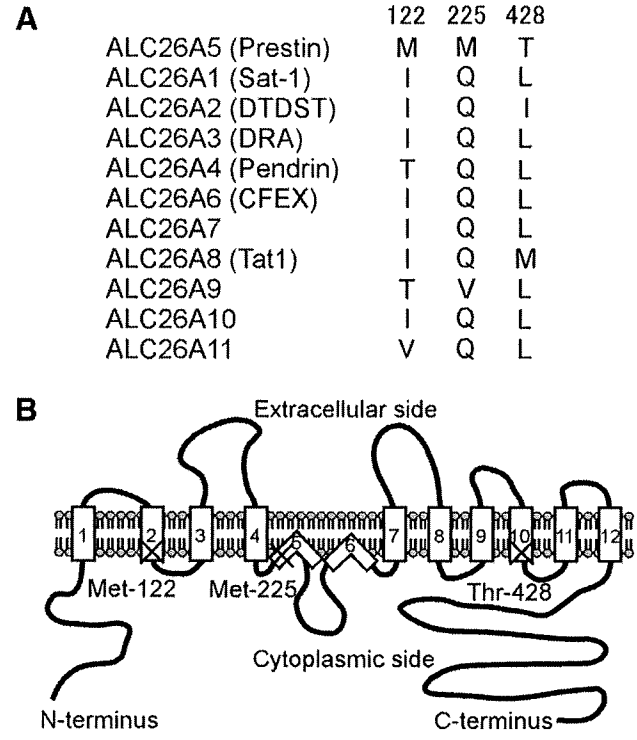

Fig. 1. Comparison of the amino acid sequences of the SLC26 proteins and the positions of the amino acids in prestin focused on in the present study. (A) Multiple alignment of the amino acid sequence of SLC26 proteins. Amino acid residue numbers refer to amino acids of prestin. Methionine was found at positions of 122 and 225 in prestin, while isoleucine and glutamine were detected at the corresponding positions of most of the other SLC26 proteins, respectively. In addition, prestin has threonine at position of 428, but most of the other SLC26 proteins have leucine at the corresponding positions. (B) Predicted membrane topology of prestin [11]. The positions of Met-122, Met-225 and Thr-428 in prestin are shown by "X" in its predicted membrane topology.

then observed using a confocal laser scanning microscope (FV500, Olympus, Tokyo, Japan). Detected TRITC fluorescence and Alexa Fluor 633 fluorescence were indicated by red and green, respectively.

In the present study, the ratio of the amount of prestin localized in the plasma membrane to the total amount of prestin in the cell, R_p, was investigated. The R_p was calculated by the following equation:

$$R_p = \frac{I_p}{I_w}, \quad (4)$$

where I_w is the summation of the intensity of TRITC fluorescence of the whole area of the target cell which reflects the total amount of prestin in the cell, and I_p is the summation of the intensity of TRITC fluorescence of only pixels corresponding to the plasma membrane, which reflects the amount of prestin there. For the calculation of I_w and I_p, the average intensity value of the background noise of TRITC fluorescence was first subtracted from the intensity value of TRITC fluorescence in all pixels in the obtained images. In the subtracted images, only pixels whose intensity values of TRITC fluorescence were 6 times greater than such background noise were used for the calculation of I_w and I_p. I_w was obtained by summing up the intensity values of TRITC fluorescence of the whole areas of the target cells in the subtracted images. To calculate I_p, the pixels which corresponded to the plasma membrane had to be defined. The plasma membrane and the Golgi body of the cells were stained by WGA-Alexa Fluor 633 conjugate in this experiment. As the plasma membrane and the Golgi body are at different positions in the cells, the positions of the pixels corresponding to the plasma membrane were identifiable. I_p was obtained by summing up the intensity values of TRITC fluorescence of the pixels corresponding to the plasma membrane which had an intensity value of Alexa Fluor 633 fluorescence 2 times greater than its background noise.

Results and discussion

As a result of the multiple alignments of the amino acid sequences of the SLC26 family proteins, we found that methionine was present at positions of 122 and 225 of prestin, but that the majority of the other SLC26 proteins had isoleucine and glutamine at the corresponding positions, respectively (Fig. 1). In addition, prestin has threonine at position of 428, but leucine was found at the corresponding positions in the majority of the other SLC26 proteins. The side chains of amino acids in prestin described above have different characteristics from those of the corresponding amino acids in the other SLC26 proteins. Thus, Met-122, Met-225 and Thr-428 of prestin were considered to be unique in the SLC26 family, therefore implying that they are responsible for the unique functions of prestin. In the present study, to clarify roles of Met-122, Met-225 and Thr-428 in prestin, mutations were introduced into those amino acids, resulting in three prestin mutants, namely, M122I, M225Q and T428L. Characteristics of those prestin mutants were then investigated.

Fig. 2 shows recorded NLC curves and the fitting parameters obtained in WT-expressing cells and prestin mutant-expressing cells. In addition to WT, all mutants prepared in the present study showed NLC (Fig. 2A). Compared with the $V_{1/2}$ of WT, that of M122I and M225Q and that of T428L were statistically shifted in the hyperpolarization and depolarization direction, respectively ($p < 0.05$) (Fig. 2B). In addition, T428L showed a statistically smaller α than that of WT ($p < 0.05$) (Fig. 2C). The changes in the $V_{1/2}$ and α indicate changes in the reactivity of prestin to the membrane

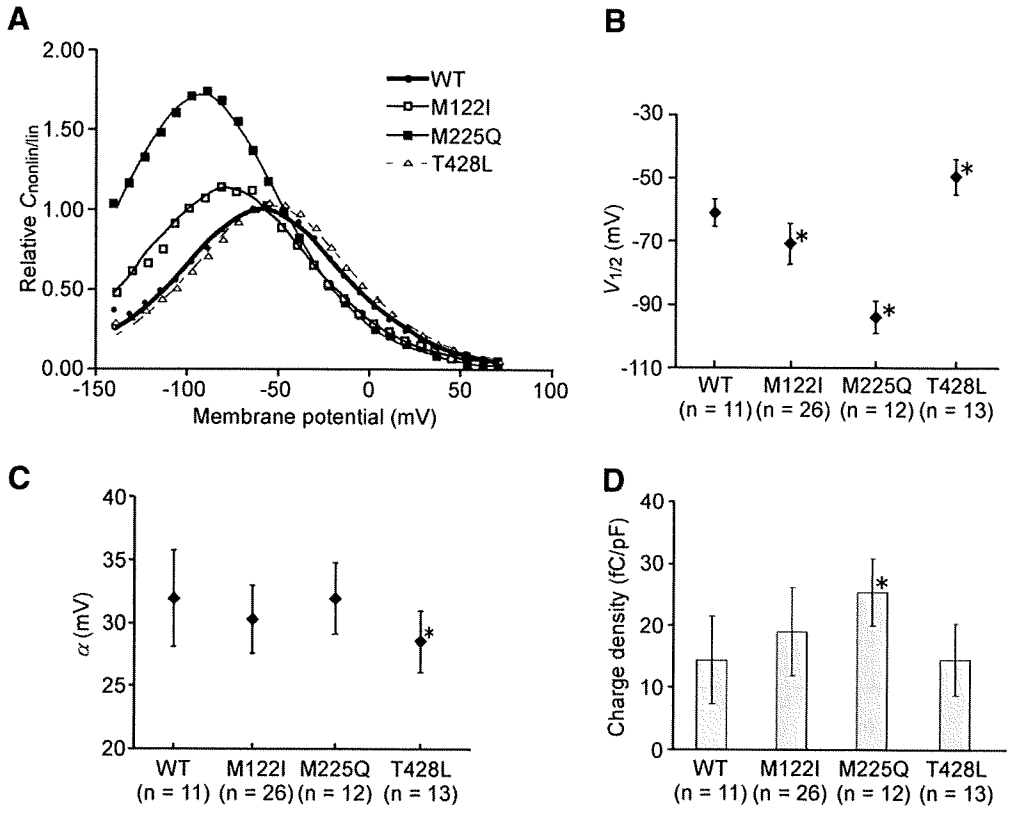

Fig. 2. Results of the whole-cell patch-clamp recording. (A) NLC curves. Not only WT but also all prestin mutants showed NLC. (B) $V_{1/2}$. M122I and M225Q and T428L showed $V_{1/2}$ statistically shifted in the hyperpolarization and depolarization direction, respectively ($p < 0.05$). (C) α. The α of T428L was statistically smaller than that of WT ($p < 0.05$). (D) Charge density. Interestingly, M225Q showed statistically larger charge density than that of WT ($p < 0.05$). In contrast, there was no statistical difference between WT and the other mutants.

potential and anions. As methionine and threonine do not have charge, the mutations of Met-122, Met-225 and Thr-428 might affect the structure of prestin, but not as greatly as the abolishment of NLC, and thus alter such reactivity. As shown in Fig. 2D, the charge density of M122I and T428L was similar to that of WT, suggesting that Met-122 and Thr-428 are not required for the generation of NLC. On the other hand, interestingly, the charge density of M225Q was significantly larger than that of WT ($p < 0.05$). To confirm if the motility of prestin-expressing cells was also increased by the mutation in Met-225, that motility was measured in the microchamber configuration. Results showed that the displacement of M225Q-expressing cells due to the variation in the membrane potential was statistically greater than that of WT-expressing cells ($p < 0.05$) (Fig. 3), suggesting that the replacement of Met-225 by glutamine significantly enhanced the charge density and the motility of prestin-expressing cells. This result implies that one reason why prestin has methionine instead of glutamine at position 225 may be to somehow adjust the charge density and the motility of prestin-expressing cells.

To understand the contributions of Met-225 to prestin in more detail, the mechanism of the increase in the charge density and the motility of prestin-expressing cells by the mutation in Met-225 were investigated. First, the amount of M225Q and WT in the cells was analyzed by comparing the band intensity of M225Q with that of WT in Western blotting (Fig. 4A and B). No statistical difference in the band intensity was detected between WT and M225Q, suggesting that the amount of M225Q in the cells was similar to that of WT. In addition, the localization of M225Q in the cells was compared with that of WT by immunofluorescence staining. Fig. 4C and D shows representative images of stained cells and R_p, which is the ratio of the amount of prestin in the plasma membrane to the total amount of prestin in the cells. The R_p of M225Q was similar to that of WT, meaning that the localization pattern was unchanged by the mutation in Met-225. Thus, the replacement of Met-225 by glutamine was found not to change the amount of prestin and its localization pattern in the cells.

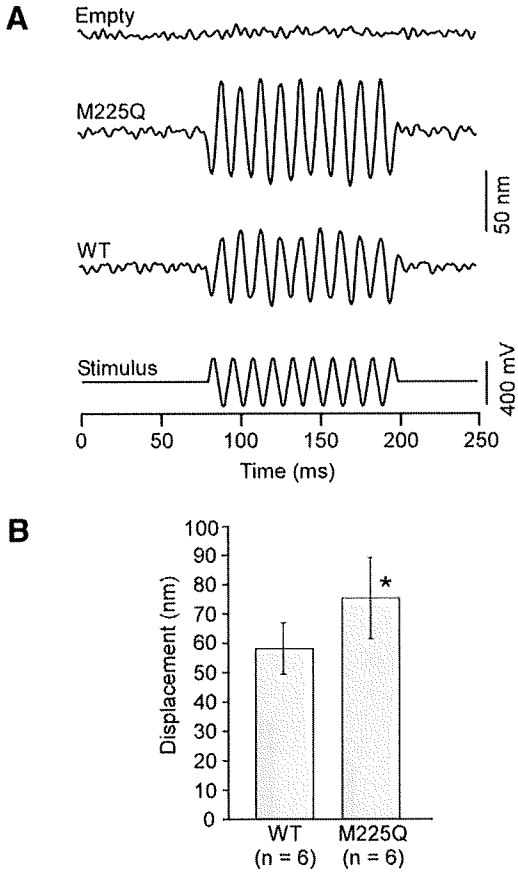

Fig. 3. Motile response of WT-expressing cells and M225Q-expressing cells. (A) Results of measurement of the motility of prestin-expressing cells. Unlike empty vector-transfected cells, WT-expressing cells and M225Q-expressing cells exhibited motile response to changes in their membrane potential. (B) Comparison of the displacement of WT-expressing cells and M225Q-expressing cells. The displacement of M225Q-expressing cells was statistically larger than that of WT-expressing cells ($p < 0.05$).

In the present study, we found that the charge density and the motility of prestin-expressing cells statistically increased by the mutation in Met-225, but that the amount of prestin and its localization pattern in the cells remained unchanged. This means that such increase cannot be explained by the increase of the amount of prestin in the plasma membrane. Due to uniqueness of our results, they might be considered to be implausible. However, the observed interesting phenomena, namely, the increase in the charge density of prestin-expressing cells without an increase of prestin in the plasma membrane, has been found so far in conditions different from those of the present study. Oliver et al. [18] showed that in the inside-out patch-clamp recording for OHCs, Q_{max} increased by changing anions from Cl^- to I^- in the solution on the cytoplasmic surface of the membrane. The increase of Q_{max} in the inside-out patch-clamp recording has the same meaning as the increase of the charge density because in such recording, C_{lin} is almost constant between the samples and the charge density is calculated by the division of Q_{max} by C_{lin}. In inside-out patch-clamp recording, it is unlikely that the amount of prestin in the plasma membrane increases during such recording. That is, in the study of Oliver et al., the charge density increased without an increase in the amount of prestin in the plasma membrane. Moreover, Deák et al. [11] showed that the charge density increased when N^2,2′-*O*-dibutyrylguansine 3′,5′-cyclic monophosphate sodium salt hydrate (DBcGMP), which induces the phosphorylation of prestin, was contained in the patch pipette in the whole-cell patch-clamp recording. Such increase was recordable from 5 s after establishment of the whole-cell patch-clamp configuration, ruling out the possibility that the increase of the charge density resulted from the increase in the amount of prestin in the plasma membrane caused by DBcGMP because 5 s was insufficient for the translocation of proteins caused by cGMP [19]. Thus, those two studies showed that it was possible that the charge density increased by some manipulations without the increase in the amount of prestin in the plasma membrane, enhancing the credibility of our interesting results. To interpret our study and two studies mentioned above, it should be considered that both functional and non-functional prestin exist in the plasma membrane. If the ratio of the amount of functional prestin to the total amount of functional and non-functional prestin in the plasma membrane increases, the charge density and the motility of prestin-expressing cells can increase without an increase in the total amount of these two types of prestin. The study of Oliver et al. may indicate that as the amount of prestin interacting with I^- is larger than that of prestin interacting with Cl^- in the plasma membrane, changing anions from Cl^- to I^- led to the increase in the amount of prestin interacting with anions, namely, the increase of the amount of functional prestin in the plasma membrane. The study of Deák et al. may mean that the phosphorylation of prestin somehow increased the ratio of the amount of functional prestin to the total amount of functional and non-functional prestin in the plasma membrane. Also in the present study, the replacement of Met-225 by glutamine was speculated to increase such ratio, resulting in the increase in the charge density as well as in the motility of prestin-expressing cells, which implies that Met-225 adjusts the charge density and the motility, probably by controlling such ratio.

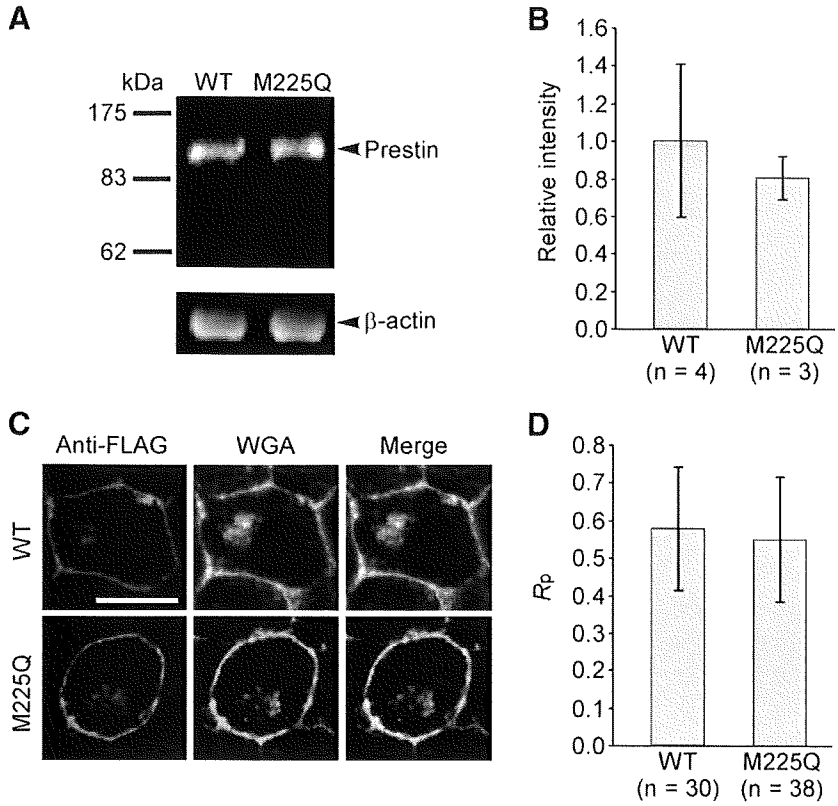

Fig. 4. Amount of prestin and its localization in the cells. (A) Western blotting using whole-cell lysate of prestin-expressing cells. The 100 kDa bands were found in both WT and M225Q. (B) Comparison of the intensity of bands. The intensity of bands of WT and M225Q was normalized by that of β-actin bands, and then relative intensity was obtained by dividing the normalized intensity of the WT band and that of the M225Q band by the average of the normalized intensity of the WT band. There was no statistical difference in the relative intensity between WT and M225Q. (C) Representative images of a stained WT-expressing cell and a M225Q-expressing cell. Red fluorescence indicates prestin and green indicates the plasma membrane and the Golgi body. In merged images, orange-yellow fluorescence shows the co-localization of prestin and the plasma membrane and that of prestin and the Golgi body, scale bar shows 10 μm. (D) Ratio of the amount of prestin localized in the plasma membrane to the total amount of prestin in the cell, R_p. The R_p of M225Q was similar to that of WT, indicating that the localization pattern was unchanged by the mutation.

In summary, we introduced point mutations into the unique amino acids in prestin, Met-122, Met-225 and Thr-428. As a result, the replacement of Met-225 in prestin by glutamine was found to remarkably increase the charge density and the motility of prestin-expressing cells without an increase of prestin in the plasma membrane, implying that Met-225 in prestin somehow adjusts the charge density and the motility. In addition, our results showed that Met-122 and Thr-428 are not required for prestin to confer cells with NLC.

Acknowledgments

This work was supported by Grant-in-Aid for Scientific Research (B) 18390455 from the Japan Society for the Promotion of Science, by Grant-in-Aid for Exploratory Research 18659495 from the Ministry of Education, Culture, Sports, Science and Technology of Japan, by a grant from the Human Frontier Science Program, by a Health and Labour Science Research Grant from the Ministry of Health, Labour and Welfare of Japan and by Tohoku University Global COE Program "Global Nano-Biomedical Engineering Education and Research Network Centre" to H.W., and by a Grant-in-Aid for JSPS Fellows from the Japan Society for the Promotion of Science to S.K.

References

[1] J. Zheng, W. Shen, D.Z.Z. He, K.B. Long, L.D. Madison, P. Dallos, Prestin is the motor protein of cochlear outer hair cells, Nature 405 (2000) 149–155.
[2] P. Dallos, B. Fakler, Prestin, a new type of motor protein, Nat. Rev. Mol. Cell Biol. 3 (2002) 104–111.
[3] J. Ludwig, D. Oliver, G. Frank, N. Klöcker, A.W. Gummer, B. Fakler, Reciprocal electromechanical properties of rat prestin: the motor molecule from rat outer hair cells, Proc. Natl. Acad. Sci. USA 98 (2001) 4178–4183.
[4] D.B. Mount, M.F. Romero, The SLC26 gene family of multifunctional anion exchangers, Pflugers Arch. 447 (2004) 710–721.
[5] J. Santos Sacchi, Reversible inhibition of voltage-dependent outer hair cell motility and capacitance, J. Neurosci. 11 (1991) 3096–3110.
[6] J. Zheng, G.G. Du, K. Matsuda, A. Orem, S. Aguiñaga, L. Deák, E. Navarrete, L.D. Madison, P. Dallos, The C-terminus of prestin influences nonlinear capacitance and plasma membrane targeting, J. Cell Sci. 118 (2005) 2987–2996.
[7] D. Navaratnam, J.P. Bai, H. Samaranayake, J. Santos Sacchi, N-terminal-mediated homomultimerization of prestin, the outer hair cell motor protein, Biophys. J. 89 (2005) 3345–3352.
[8] J.P. Bai, D. Navaratnam, H. Samaranayake, J. Santos Sacchi, En block C-terminal charge cluster reversals in prestin (SLC26A5): effects on voltage-dependent electromechanical activity, Neurosci. Lett. 404 (2006) 270–275.
[9] L. Rajagopalan, N. Patel, S. Madabushi, J.A. Goddard, V. Anjan, F. Lin, C. Shope, B. Farrell, O. Lichtarge, A.L. Davidson, W.E. Brownell, F.A. Pereira, Essential helix interactions in the anion transporter domain of prestin revealed by evolutionary trace analysis, J. Neurosci. 26 (49) (2006) 12727–12734.
[10] K. Matsuda, J. Zheng, G.G. Du, N. Klöcker, L.D. Madison, P. Dallos, N-linked glycosylation sites of the motor protein prestin: effects on membrane targeting and electrophysiological function, J. Neurochem. 89 (2004) 928–938.
[11] L. Deák, J. Zheng, A. Orem, G.G. Du, S. Aguiñaga, K. Matsuda, P. Dallos, Effects of cyclic nucleotides on the function of prestin, J. Physiol. 563 (2005) 483–496.
[12] K. Mio, Y. Kubo, T. Ogura, T. Yamamoto, F. Arisaka, C. Sato, The motor protein prestin is a bullet-shaped molecule with inner cavities, J. Biol. Chem. 283 (2007) 1137–1145.
[13] M. Murakoshi, K. Iida, S. Kumano, H. Wada, Immune atomic force microscopy of prestin-transfected CHO cells using quantum dots, Pflugers Arch. 457 (2009) 885–898.
[14] M.A. Larkin, G. Blackshields, N.P. Brown, R. Chenna, P.A. McGettigan, H. McWilliam, F. Valentin, I.M. Wallace, A. Wilm, R. Lopez, J.D. Thompson, T.J. Gibson, D.G. Higgins, Clustal W and Clustal X version 2.0, Bioinformatics 23 (2007) 2947–2948.

[15] K. Iida, K. Tsumoto, K. Ikeda, I. Kumagai, T. Kobayashi, H. Wada, Construction of an expression system for the motor protein prestin in Chinese hamster ovary cells, Hear. Res. 205 (2005) 262–270.
[16] D.Z.Z. He, B.N. Evans, P. Dallos, First appearance and development of electromotility in neonatal gerbil outer hair cells, Hear. Res. 78 (1994) 77–90.
[17] P. Dallos, N.E. Evans, R. Hallworth, Nature of the motor element in electrokinetic shape changes of cochlear outer hair cells, Nature 350 (1991) 155–157.
[18] D. Oliver, D.Z.Z. He, N. Klöcker, J. Ludwig, U. Schulte, S. Waldegger, J.P. Ruppersberg, P. Dallos, B. Fakler, Intracellular anions as the voltage sensor of prestin, the outer hair cell motor protein, Science 292 (2001) 2340–2343.
[19] S. Komatsu, K. Miyazaki, R.A. Tuft, M. Ikebe, Translocation of telokin by cGMP signaling in smooth muscle cells, Am. J. Physiol. Cell Physiol. 283 (2002) C752–C761.